Power Allocation and Error Performance of Distributed Unitary Space–Time Modulation in Wireless Relay Networks

Duy H. N. Nguyen, *Student Member, IEEE*, Ha H. Nguyen, *Senior Member, IEEE*, and Hoang Duong Tuan, *Member, IEEE*

***Abstract*—A wireless relay network allows relays to cooperate with each other, emulate a virtual array of transmit antennas, and perform distributed space–time modulation of the source signals. In this paper, two types of relay networks are considered—one with no channel state information (CSI) (i.e., the noncoherent networks) and one with only the information of the relay-to-destination channels (i.e., the partially coherent networks) at the destination. First, a new optimal power-allocation (PA) scheme is derived to maximize the average signal-to-noise ratio (SNR) at the destination while minimizing the amount of fading experienced over the network. Second, the Fourier-based unitary space–time modulation (USTM), which was originally proposed for multiple colocated transmit antennas, is applied to wireless relay networks. The receivers for such distributed USTM over noncoherent and partially coherent networks are developed, and their error performances are shown to be asymptotically the same. The impact of different PA schemes on the error performance of distributed USTM is thoroughly illustrated with simulation results.**

***Index Terms*—Amount of fading, distributed space–time coding (DSTC), power allocation (PA), unitary space–time modulation (USTM), wireless relay networks.**

I. Introduction

THE CONCEPT of cooperation in communications [1]–[5] has recently drawn much research attention due to its potential to improve the efficiency of wireless networks. In cooperative communications, users can cooperate to relay each other's information signals, create a virtual array of transmit antennas, and, thus, achieve spatial diversity. Such *virtual antenna arrays* can dramatically improve the reliability of signal transmission from each user [4] and the network throughput [1]–[3]. In [3]–[7], a new cooperative strategy, which is referred to as "distributed space–time coding" (DSTC), was proposed, where the conventional space–time coding for colocated antennas is implemented among the users (or relays) in a distributed manner. Yiu *et al.* [8] presented a new type of distributed space–time block codes (DSTBCs) for wireless networks with a large number of users, where each user is assigned a unique signature vector.

While most of the works on cooperative communications in the literature assume the availability of perfect channel state information (CSI) of all the channels at the relays and/or destination, a few of them have considered the scenarios where only imperfect channel estimation or no CSI is available. Differential modulation scheme for a two-user cooperative system was discussed in [9], whereas a noncoherent energy detector for binary frequency-shift keying signaling with a piecewise linear combiner was considered in [10]. Reference [11] investigated the noncoherent and mismatched coherent detectors for distributed STBC with one relay, where it is shown that the system can achieve a diversity order of 2. However, the derivations [11, eqs. (19) and (20)] for the suboptimal receiver in the noncoherent detection turn the problem into the partially coherent one. The partially coherent relay network was investigated in detail in [12], where a differential coding scheme was proposed to take advantage of the cooperative diversity. For noncoherent relay networks, a fully diverse distributed coding scheme based on division algebra was proposed in [13] and [14]. Similar to the work in [6], references [12]–[14] consider amplify-and-forward (AF) protocol with linear processing at the relays.

Noncoherent reception for DSTC was also proposed in [15], where the decode-and-forward (DF), selection relaying (SR), incremental DF, and incremental SR protocols were employed, and unitary space–time modulation (USTM) was implemented in a distributed fashion among the relays. A similar approach using the DF protocol was also reported in [8] and [16]. However, the drawback with these approaches is that the relay only forwards if it decodes the source signal correctly in the SR protocol, or it always forwards in the DF protocol. Given the random nature of the channels in wireless relay networks, for instance, when the channels between the source and some of the relays are bad, it is highly probable that the relays would decode incorrectly and, thus, would not forward in the SR protocol or would forward the incorrect version of the source signal in the DF protocol. This will compromise the diversity advantage of DSTC. Moreover, the incremental DF and incremental SR require feedback from the destination to all the

Manuscript received July 23, 2008; revised November 6, 2008. First published January 27, 2009; current version published August 14, 2009. The work of the first and second authors was supported by a Natural Sciences and Engineering Research Council Discovery Grant. The work of the third author was supported by an Australian Research Council Discovery Grant. The review of this paper was coordinated by Dr. M. Dohler.

D. H. N. Nguyen and H. H. Nguyen are with the Department of Electrical Engineering, University of Saskatchewan, Saskatoon, SK S7N 5A9, Canada (e-mail: duy.nguyen@usask.ca; ha.nguyen@usask.ca).

H. D. Tuan is with the School of Electrical Engineering and Telecommunications, University of New South Wales, Sydney, NSW 2052, Australia (e-mail: h.d.tuan@unsw.edu.au).

Digital Object Identifier 10.1109/TVT.2009.2013631

relays. The AF protocol is generally preferred over other protocols since it is always able to achieve the maximum diversity order and feedback from the destination is not required.

Power allocation (PA) is also an important issue in designing wireless relay networks. Given a limited power budget, it is necessary to optimize the transmit power at all nodes, including the source and relays, under some performance criterion. Distributed adaptive PA for relay networks was first studied in [17] for both AF and DF protocols, in which the authors proposed an optimal PA scheme that significantly increases the signal-to-noise ratio (SNR) at the destination over the equal PA. It is noted, however, that the optimal PA for DSTC [6], [12]–[14] in an arbitrary relay network has not been fully studied.

This paper focuses on wireless relay networks with the AF protocol. Two types of wireless relay networks are considered—one with no CSI (i.e., the noncoherent networks) and one with only the information of the relay-to-destination channels (i.e., the partially coherent networks) at the destination. The main contributions of this paper are as listed follows. First, this paper shows that in maximizing the average SNR at the destination, it is possible that not all the relays are active.[1] The optimal PA to the active relay(s) is also obtained. The amount of fading is then introduced to the relay networks and is used as a constraint to derive a novel optimal PA scheme. Not only does this scheme maximize the effective average SNR at the destination, where the relays can be anywhere between the source and the destination, but it also leverages the fading of each source–relay–destination ($S \to R \to D$) link. Second, it shows how to incorporate the Fourier-based USTM into wireless relay networks in a distributed manner. Developed are the maximum likelihood (ML) receiver for the distributed USTM (DUSTM) over partially coherent relay networks and the generalized likelihood ratio test (GLRT) receiver for the noncoherent relay networks. Performance comparison of the DUSTM over the two types of relay networks reveals that although the knowledge of relay-to-destination channels improves the symbol error rate (SER) compared with the case of fully noncoherent networks, this advantage diminishes as the total system power becomes large enough. In fact, it is shown that their performances are asymptotically the same when all the relays are active. Full diversity order equal to the number of relays is achievable in both networks if the coherence time is larger than twice the number of relays.

Notations: Superscripts $(\cdot)^{\mathcal{T}}$, $(\cdot)^*$, and $(\cdot)^{\mathcal{H}}$ stand for transpose, complex conjugate, and complex conjugate transpose operations, respectively; $\boldsymbol{I}_M$ stands for the $M \times M$ identity matrix; $\mathrm{diag}(d_1, d_2, \ldots, d_M)$ denotes an $M \times M$ diagonal matrix with diagonal entries $d_1, d_2, \ldots, d_M$; $\det(\cdot)$ and $\mathrm{tr}(\cdot)$ denote the determinant and the trace of a square matrix; $\mathbb{E}_x[\cdot]$ and $\mathrm{var}_x[\cdot]$ indicate the expectation and variance of random variable x, respectively; and $\mathcal{CN}(0, \sigma^2)$ denotes a circularly symmetric Gaussian random variable with variance σ^2.

[1]Hereafter, a relay is said to be "active" if it is distributed a nonzero power by the PA scheme. Otherwise, the relay is said to be "inactive."

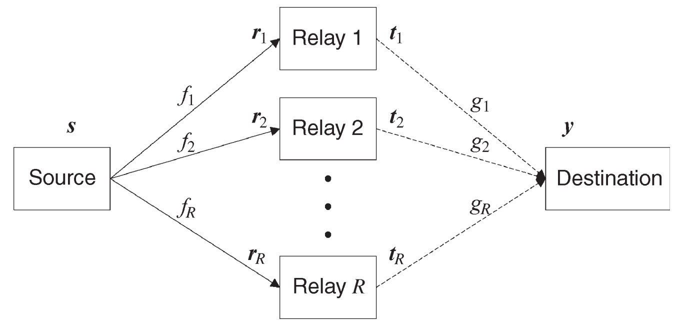

Fig. 1. Block diagram of distributed space–time modulation in a wireless relay network with $R+2$ nodes.

II. System Model

Consider a wireless relay network with $R+2$ nodes, as illustrated in Fig. 1. The system has one source node, one destination node, and R relay nodes. Each node is equipped with only one antenna, which can be used for both reception and transmission. The relays are assumed to work in the half-duplex mode, i.e., they cannot receive and transmit signals simultaneously. Assume that there is no direct link from the source to the destination as signals from the source are relayed to arrive at the destination. It is further assumed that all the channels from the source to the relays and from the relays to the destination have the coherence time longer than T.

Let $\mathcal{S} = \{\boldsymbol{s}_1, \ldots, \boldsymbol{s}_L\}$ be the codebook consisting of L distinguished codewords of length T employed by the source, where $\boldsymbol{s}_l^{\mathcal{H}} \boldsymbol{s}_l = 1$, for $l = 1, \ldots, L$. In the first stage, the source transmits the vector $\sqrt{P_0 T}\boldsymbol{s}$ over T symbol intervals such that P_0 is the average power per transmission. Every relay listens to the transmitted signal from the source. The received signal at relay i can be written as

$$\boldsymbol{r}_i = \sqrt{P_0 T} f_i \boldsymbol{s} + \boldsymbol{w}_{R_i} \qquad (1)$$

where f_i is the channel coefficient between the source and the ith relay, which is modeled as $\mathcal{CN}(0, \sigma_{F_i}^2)$. The noise vector $\boldsymbol{w}_{R_i}$ contains independent identically distributed (i.i.d.) $\mathcal{CN}(0, N_0)$ random variables.

The AF protocol [2] with linear signal processing is used at each relay. In particular, similar to [6], a *unitary relay matrix* $\boldsymbol{A}_i$ of size $T \times T$ is used to linearly process the received signal at the ith relay. Then, the transmitted signal at the ith relay can be written as

$$\boldsymbol{t}_i = \sqrt{\frac{P_i}{P_0\sigma_{F_i}^2 + N_0}} \boldsymbol{A}_i \boldsymbol{r}_i = \sqrt{\varepsilon_i} \boldsymbol{A}_i \boldsymbol{r}_i, \qquad i = 1, \ldots, R \qquad (2)$$

where the normalization factor $\varepsilon_i = P_i/(P_0\sigma_{F_i}^2 + N_0)$ maintains the average transmitted power of P_i at the ith relay. Let $g_i \sim \mathcal{CN}(0, \sigma_{G_i}^2)$ be the channel coefficient from the ith relay to the destination, and let $\boldsymbol{w}$, whose elements are i.i.d. $\mathcal{CN}(0, N_0)$, represent the additive white Gaussian noise vector. With perfectly synchronized transmissions from the relays, the received signal at the destination can be expressed as

$$\boldsymbol{y} = \sum_{i=1}^{R} g_i \boldsymbol{t}_i + \boldsymbol{w}_D = \boldsymbol{X}\boldsymbol{h} + \boldsymbol{w} \qquad (3)$$

where

$$\begin{aligned}\boldsymbol{X} &= [\boldsymbol{A}_1\boldsymbol{s},\ldots,\boldsymbol{A}_R\boldsymbol{s}]\\ \boldsymbol{h} &= \left[\sqrt{\varepsilon_1 P_0 T} f_1 g_1,\ldots,\sqrt{\varepsilon_R P_0 T} f_R g_R\right]^{\mathcal{T}}\\ \boldsymbol{w} &= \sum_{i=1}^{R}\sqrt{\varepsilon_i} g_i \boldsymbol{A}_i \boldsymbol{w}_{R_i} + \boldsymbol{w}_D. \end{aligned} \quad (4)$$

It is assumed that the fading coefficients $\{f_i\}_{i=1}^R$ and $\{g_i\}_{i=1}^R$ and the noise vectors $\{\boldsymbol{w}_{R_i}\}_{i=1}^R$ and $\boldsymbol{w}_D$ are independent of each other. Since $\boldsymbol{w}_{R_i}$ is circularly symmetric and $\boldsymbol{A}_i$ acts as a rotation matrix, the rotated noise vector $\boldsymbol{A}_i\boldsymbol{w}_{R_i}$ has the same distribution as that of $\boldsymbol{w}_{R_i}$. The average noise power can be calculated as

$$\gamma = \mathbb{E}\left[\|\boldsymbol{w}\|^2\right] = N_0\left(1+\sum_{i=1}^{R}\varepsilon_i|g_i|^2\right). \quad (5)$$

On the other hand, the *instantaneous* signal power is

$$\rho = \frac{1}{R}\sum_{i=1}^{R}\varepsilon_i P_0 T|f_i|^2|g_i|^2 = \frac{P_0 T}{R}\sum_{i=1}^{R}\varepsilon_i|f_i|^2|g_i|^2. \quad (6)$$

Accordingly, the *instantaneous* SNR at the destination is ρ/γ. Thus, the *exact* average SNR can be calculated by averaging ρ/γ over random variables $\{g_i\}_{i=1}^R$ and $\{f_i\}_{i=1}^R$ as follows:

$$\begin{aligned}\eta &= \mathbb{E}_{\{g_i\}_{i=1}^R,\{f_i\}_{i=1}^R}\left[\frac{\rho}{\gamma}\right]\\ &= \frac{P_0 T}{RN_0}\mathbb{E}_{\{g_i\}_{i=1}^R}\left[\frac{\sum_{i=1}^R \varepsilon_i\sigma_{F_i}^2|g_i|^2}{1+\sum_{i=1}^R\varepsilon_i|g_i|^2}\right]\\ &= \frac{P_0 T}{RN_0}\int_0^\infty\cdots\int_0^\infty \frac{\sum_{i=1}^R \varepsilon_i\sigma_{F_i}^2\sigma_{G_i}^2\lambda_i}{1+\sum_{i=1}^R\varepsilon_i\sigma_{G_i}^2\lambda_i}\\ &\quad\times e^{-\lambda_1},\ldots,e^{-\lambda_R}d\lambda_1,\ldots,d\lambda_R. \end{aligned} \quad (7)$$

Note that the integral follows from the fact that $|g_i|^2$ is exponentially distributed with mean $\sigma_{G_i}^2$, while the variable change $\lambda_i = |g_i|^2/\sigma_{G_i}^2$ makes λ_i exponentially distributed with mean 1. Although the exact average SNR can be evaluated numerically by the Gauss–Laguerre integration method [18], a closed-form expression of η in (7) is hard to obtain. Instead, the following approximation of η, which resulted by taking the first term of the Taylor series expansion of the expectation in (7) [19], shall be considered:

$$\eta \approx \frac{\mathbb{E}_{\{g_i\}_{i=1}^R,\{f_i\}_{i=1}^R}[\rho]}{\mathbb{E}_{\{g_i\}_{i=1}^R,\{f_i\}_{i=1}^R}[\gamma]} = \frac{P_0 T}{RN_0}\frac{\sum_{i=1}^R\varepsilon_i\sigma_{F_i}^2\sigma_{G_i}^2}{1+\sum_{i=1}^R\varepsilon_i\sigma_{G_i}^2}. \quad (8)$$

Let $P=\sum_{i=0}^R P_i$ be the total transmitted power spent in the network. It is observed that increasing P makes the average SNR at the destination higher. However, it is not clear how the total power between the source and the relays is split to maximize the average SNR. Such a PA problem is analyzed in Section III, where the approximation of η in (8) is used as the objective function. Numerical results presented in Section VI confirm the accuracy of the approximate SNR in (8) under all the PA schemes proposed and examined in this paper.

III. Optimal PA

As discussed before, the aim of PA between the source and the relays is to maximize the average SNR at the destination, given that the total power consumption $\sum_{i=0}^R P_i$ is not greater than the power budget P. Note that as the channel information is not available at neither the source nor the relays, we can only optimize the average SNR based on the channel statistics. From (8), the problem of maximizing the average SNR is equivalent to

$$\begin{aligned}\underset{P_0,\ldots,P_R}{\text{minimize}}\quad & f(P_0,\ldots,P_R) = \frac{1+\sum_{i=1}^R\frac{P_i\sigma_{G_i}^2}{P_0\sigma_{F_i}^2+N_0}}{P_0\sum_{i=1}^R\frac{P_i\sigma_{F_i}^2\sigma_{G_i}^2}{P_0\sigma_{F_i}^2+N_0}}\\ \text{subject to}\quad & \sum_{i=0}^R P_i\le P,\quad P_i\ge 0,\qquad i=0,\ldots,R. \end{aligned} \quad (9)$$

The objective function of the aforementioned optimization problem is nonconvex. However, if the source's transmitted power P_0 is fixed, the objective function is linear-fractional with respect to the relaying powers $P_1,\ldots,P_R$. Thus, the optimization problem is just a linear-fractional program, which is a subclass of convex programming [20]. Before stating the solution to (9), Lemma 1 is first presented as it is useful to establish the analytically closed-form expression of the optimal PA scheme.

Lemma 1: At the optimal solution to the optimization problem [see (9)*], the inequality* $\sum_{i=0}^R P_i\le P$ *is met with equality.*

Proof: If P_i^* is the optimal solution with $\sum_{i=0}^R P_i^* < P$, increasing P_0^* up to $P-\sum_{i=1}^R P_i^*$ makes the objective function strictly smaller, which contradicts the optimality of P_i^*. This is because the objective function is a monotonically decreasing in P_0, which follows from the fact that its numerator $1+\sum_{i=1}^R(P_i\sigma_{G_i}^2/(P_0\sigma_{F_i}^2+N_0))$ is monotonically decreasing in P_0 while its denominator $P_0\sum_{i=1}^R(P_i\sigma_{F_i}^2\sigma_{G_i}^2/(P_0\sigma_{F_i}^2+N_0)) = \sum_{i=1}^R(P_i\sigma_{F_i}^2\sigma_{G_i}^2/(\sigma_{F_i}^2+N_0/P_0))$ is monotonically increasing in P_0. ■

In [6], the optimal PA for the case of $\sigma_{F_i}^2=\sigma_{G_i}^2=1$, $i=1,\ldots,R$, was given. The allocation, which is referred to as "equal PA" in this paper, assigns half of the total power to the source and equally divides the other half to all the relays. However, the condition of $\sigma_{F_i}^2=\sigma_{G_i}^2=1$ loosely implies that all the relays are in the midway between the source and the destination. We now examine more general cases of network topology, as summarized in Table I. For convenience, hereafter, a relay network is classified as balanced if $\sigma_{F_1}^2=\cdots=\sigma_{F_R}^2$ and $\sigma_{G_1}^2=\cdots=\sigma_{G_R}^2$. Otherwise, it is classified as unbalanced. The first network considered is a balanced network, where equal power sharing at the relays is assumed and joint power optimization between the source and the relays is performed. For the second network topology, which is unbalanced, we first fix the source power P_0 and then prove that the remaining power is allocated only

TABLE I
NETWORK CONFIGURATIONS AND OPTIMIZATION PROBLEMS

Network Configuration	Optimization Problem
Balanced network	Equal power sharing at relays, joint optimization between the source and relays.
Unbalanced network	Fix source power P_0, relay power allocated to the best relay(s).
Unbalanced network with the amount of fading constraint	Balance the network by the amount of fading constraint, joint optimization between the source and the relays.

to the best relay(s). We then introduce the "amount of fading" concept into the relay networks to balance $S \to R \to D$ links. Taking into account the amount of fading constraint, a closed-form expression for the joint power optimization between the source and the relays is established.

A. Optimal PA in Balanced Networks

For a balanced network, the "average qualities" of $S \to R \to D$ links are the same. Thus, the relay power is equally shared between the relays, and the optimization problem reduces to how the power budget between the source and the relays should be distributed. Denote σ_F^2 and σ_G^2 as the common variances for $S \to R$ and $R \to D$ channels, respectively. Substituting $P_1 = \cdots = P_R = (P - P_0)/R$ into (8), the optimal PA problem is equivalent to

$$\begin{aligned} &\underset{P_0}{\text{minimize}} \quad f(P_0) = \frac{(P-P_0)\sigma_G^2 + P_0\sigma_F^2 + N_0}{P_0(P-P_0)\sigma_F^2\sigma_G^2} \\ &\text{subject to} \quad 0 < P_0 < P. \end{aligned} \tag{10}$$

In the special case of $\sigma_F^2 = \sigma_G^2$, (10) returns to the same problem in [6], and $P_0 = P/2$ and $P_1 = \cdots = P_R = (P/2R)$ constitute the optimal allocation scheme. If $\sigma_F^2 \neq \sigma_G^2$, it is simple to verify that the second-order derivative of $f(P_0)$ is always positive. Thus, $f(P_0)$ is a convex function for $0 < P_0 < P$. It is then straightforward to obtain the optimal value of P_0 from the first-order derivative of $f(P_0)$. The solution is

$$\begin{aligned} P_0 &= \begin{cases} \frac{\sqrt{\left(P\sigma_F^2+N_0\right)\left(P\sigma_G^2+N_0\right)}-\left(P\sigma_G^2+N_0\right)}{\sigma_F^2-\sigma_G^2}, & \text{if } \sigma_F^2 \neq \sigma_G^2 \\ P/2, & \text{if } \sigma_F^2 = \sigma_G^2 \end{cases} \\ P_1 &= \cdots = P_R = (P-P_0)/R \end{aligned} \tag{11}$$

where one can easily verify that the condition $0 < P_0 < P$ is met.

B. Optimal PA in Unbalanced Networks

The PA problem in an even more general setting than the cases previously examined is considered next. Here, $\sigma_{F_i}^2$ and $\sigma_{G_i}^2$, $i = 1, \ldots, R$ can take on any values. This consideration is more practical than that of balanced networks since there are no restrictions on the relay locations as well as the fading profiles of $S \to R$ and $R \to D$ channels.

Since the objective function in (9) is nonconvex, it may not be straightforward to directly solve the optimization problem. Let us fix P_0 and optimize the function over $P_1, \ldots, P_R$ first. This is equivalent to fixing the source's transmitted power and optimizing the PA between the relays. We later optimize the objective function over P_0 to yield the optimal solution. The optimization problem (9) can be rewritten as

$$\begin{aligned} &\underset{\boldsymbol{x}}{\text{minimize}} \quad f_1(\boldsymbol{x}) = \frac{1}{\boldsymbol{p}^{\mathcal{T}}\boldsymbol{x}} + \frac{\boldsymbol{q}^{\mathcal{T}}\boldsymbol{x}}{\boldsymbol{p}^{\mathcal{T}}\boldsymbol{x}} \\ &\text{subject to} \quad \mathbf{1}^{\mathcal{T}}\boldsymbol{x} = P - P_0, \qquad \boldsymbol{x} \succeq 0 \end{aligned} \tag{12}$$

where

$$\begin{aligned} \boldsymbol{p} &= P_0 \left[\frac{\sigma_{F_1}^2\sigma_{G_1}^2}{P_0\sigma_{F_1}^2 + N_0}, \ldots, \frac{\sigma_{F_R}^2\sigma_{G_R}^2}{P_0\sigma_{F_R}^2 + N_0}\right]^{\mathcal{T}} \\ \boldsymbol{q} &= \left[\frac{\sigma_{G_1}^2}{P_0\sigma_{F_1}^2 + N_0}, \ldots, \frac{\sigma_{G_R}^2}{P_0\sigma_{F_R}^2 + N_0}\right]^{\mathcal{T}} \\ \boldsymbol{x} &= [P_1, \ldots, P_R]^{\mathcal{T}} \\ \mathbf{1} &= [1, \ldots, 1]^{\mathcal{T}} \in \mathbb{R}^R. \end{aligned}$$

Note that the equality constraint follows from Lemma 1.

With the variable change $\boldsymbol{z} = (\boldsymbol{x}/\boldsymbol{p}^{\mathcal{T}}\boldsymbol{x})$, which implies that $\boldsymbol{p}^{\mathcal{T}}\boldsymbol{z} = 1$ and $(1/\boldsymbol{p}^{\mathcal{T}}\boldsymbol{x}) = (\mathbf{1}^{\mathcal{T}}\boldsymbol{z}/\mathbf{1}^{\mathcal{T}}\boldsymbol{x}) = (\mathbf{1}^{\mathcal{T}}\boldsymbol{z}/P - P_0)$ whenever $\mathbf{1}^{\mathcal{T}}\boldsymbol{x} = P - P_0$, the optimization problem in (12) becomes the following linear programming:

$$\begin{aligned} &\underset{\boldsymbol{z}}{\text{minimize}} \quad \left(\frac{1}{P-P_0}\mathbf{1} + \boldsymbol{q}\right)^{\mathcal{T}} \boldsymbol{z} = \bar{\boldsymbol{q}}^{\mathcal{T}}\boldsymbol{z} \\ &\text{subject to} \quad \boldsymbol{z} \succeq 0 \quad \boldsymbol{p}^{\mathcal{T}}\boldsymbol{z} = 1 \end{aligned} \tag{13}$$

where $\bar{\boldsymbol{q}} = (1/P - P_0)\mathbf{1} + \boldsymbol{q}$.

An obvious optimal solution of the aforementioned problem is

$$\boldsymbol{z} = [0, \ldots, 0, 1/\boldsymbol{p}_i, 0, \ldots, 0]^{\mathcal{T}} \tag{14}$$

where the index i is taken such that $\bar{\boldsymbol{q}}_i/\boldsymbol{p}_i$ is minimum. Further, the corresponding optimal value of the objective function in (13) is $\bar{\boldsymbol{q}}_i/\boldsymbol{p}_i$. If there are more than one $\bar{\boldsymbol{q}}_i/\boldsymbol{p}_i$ attaining the minimum value, any distribution between the corresponding relays will result in the same optimal value of the objective function.

It can further be verified that when the relay network is balanced, $\bar{\boldsymbol{q}}_i/\boldsymbol{p}_i$ is equal for all $i = 1, \ldots, R$ and any distribution of the total relay power results in the same optimal value of the objective function, i.e., the same maximum value of the effective SNR. Nevertheless, the scheme that equally shares the power between the relays is most preferred, since it makes use of all the relays and minimizes the amount of fading experienced over the network, as introduced and discussed in more detail in Section III-C and D. This equal-PA scheme is also consistent with the previous analysis of the balanced networks.

From the aforementioned analysis, it is clear that with a fixed value of P_0, not all the relays might be active in an unbalanced network. It is of interest to find which relay(s) are active and how the total power should be distributed between the source and the active relay(s). As shown above, for a fixed source power P_0, the active relay is identified by the index, which is denoted by $i_{\rm act}(P_0)$, such that $\bar{\boldsymbol{q}}_{i_{\rm act}(P_0)}/\boldsymbol{p}_{i_{\rm act}(P_0)}$ is minimum. That is

$$i_{\rm act}(P_0) = \arg\min_{i=1,\ldots,R} \frac{\bar{\boldsymbol{q}}_i}{\boldsymbol{p}_i} = \arg\min_{i=1,\ldots,R} \frac{(P-P_0)\sigma_{G_i}^2 + P_0\sigma_{F_i}^2 + N_0}{P_0(P-P_0)\sigma_{F_i}^2\sigma_{G_i}^2}. \quad (15)$$

Note that if there are multiple minimizers in (15), those minimizers assign the corresponding multiple active relays.

Regardless of the number of active relays, the optimization of the source power can be solved by expressing the optimization problem in (9) as follows:

$$\min_{0<P_0<P}\min_{i=1,\ldots,R} \frac{(P-P_0)\sigma_{G_i}^2 + P_0\sigma_{F_i}^2 + N_0}{P_0(P-P_0)\sigma_{F_i}^2\sigma_{G_i}^2} = \min_{i=1,\ldots,R}\min_{0<P_0<P} \frac{(P-P_0)\sigma_{G_i}^2 + P_0\sigma_{F_i}^2 + N_0}{P_0(P-P_0)\sigma_{F_i}^2\sigma_{G_i}^2}. \quad (16)$$

For each $i = 1, 2, \ldots, R$, let

$$\mu_i = \min_{0<P_0<P} \frac{(P-P_0)\sigma_{G_i}^2 + P_0\sigma_{F_i}^2 + N_0}{P_0(P-P_0)\sigma_{F_i}^2\sigma_{G_i}^2}. \quad (17)$$

Observe that (17) is in the form of (10), where the common variances σ_F^2 and σ_G^2 for a balanced network are replaced by $\sigma_{F_i}^2$ and $\sigma_{G_i}^2$ for the specific $S \to R \to D$ link via the ith relay. Thus, for each i, the optimal source power, which is denoted by $P_{0,i}$, is given by

$$P_{0,i} = \begin{cases} \frac{\sqrt{\left(P\sigma_{F_i}^2+N_0\right)\left(P\sigma_{G_i}^2+N_0\right)}-\left(P\sigma_{G_i}^2+N_0\right)}{\sigma_{F_i}^2-\sigma_{G_i}^2}, & \text{if } \sigma_{F_i}^2 \neq \sigma_{G_i}^2 \\ P/2, & \text{if } \sigma_{F_i}^2 = \sigma_{G_i}^2. \end{cases} \quad (18)$$

The corresponding value of μ_i is

$$\mu_i = \begin{cases} \frac{\left(\sigma_{F_i}^2-\sigma_{G_i}^2\right)^2}{\left(\sqrt{P\sigma_{F_i}^2+N_0}-\sqrt{P\sigma_{G_i}^2+N_0}\right)^2\sigma_{F_i}^2\sigma_{G_i}^2}, & \text{if } \sigma_{F_i}^2 \neq \sigma_{G_i}^2 \\ \frac{4(P\sigma_{F_i}^2+N_0)}{P^2\sigma_{F_i}^2\sigma_{G_i}^2}, & \text{if } \sigma_{F_i}^2 = \sigma_{G_i}^2. \end{cases} \quad (19)$$

The following proposition summarizes the optimal PA for an unbalanced network.

Proposition 1: The optimal PA scheme for maximizing the effective SNR in an unbalanced relay network would spend all the relay power to the relays with the best overall $S \to R \to D$ channels. The indices of such active relays are found by $i_{\rm act} = \arg\min_{i=1,\ldots,R}\mu_i$, where μ_i is defined in (19). *Furthermore, given the index of an active relay, i.e., $i = i_{\rm act}$, the optimal source power is found in* (18). *Any distribution of the remaining power, i.e., the relay power, between the active relay(s) gives the same optimal SNR at the destination.*

It is clear from Proposition 1 that in unbalanced networks, while the optimal PA scheme maximizes the long-term average SNR at the destination, it may distribute no power to some of the relays. This may affect the error performance of the distributed code as its diversity order is reduced (since the number of independent channels in the network is reduced). Therefore, some additional constraints should be introduced into the optimization problem to ensure that all the relays are active, i.e., the relay power is allocated to all the relays, hence, providing full diversity order. In Section III-C, the amount of fading concept is introduced for the relay networks and used as an additional constraint for the PA problem. The amount of fading gives a convenient measure of the fading severity experienced by the network, and it should be kept as small as possible. It shall be shown that the amount of fading in a relay network can be reduced inversely to the number of relays. Then, the condition on the transmitted power at each relay is derived to obtain a lower bound on the amount of fading.

C. Amount of Fading in Relay Networks

The amount of fading is a common measure of fading severity in a fading channel model. In single-input–single-output communication systems, the amount of fading is defined based on the instantaneous fading amplitude $\alpha = |h|$ of the complex fading coefficient h as [21]

$$\kappa = \frac{\mathrm{var}[\alpha^2]}{(\mathbb{E}[\alpha^2])^2}. \quad (20)$$

In multiple-input–multiple-output communication systems, α^2 is the summation of the instantaneous squared magnitudes of all the channel coefficients between each pair of transmit and receive antennas [22]. In the distributed space–time relay network considered in this paper, by taking into account the fading coefficients in each $S \to R \to D$ link, α^2 can be loosely defined as

$$\alpha^2 = \sum_{i=1}^{R} \frac{P_i|f_i|^2|g_i|^2}{P_0\sigma_{F_i}^2 + N_0}. \quad (21)$$

By disregarding common factors, the amount of fading of the considered relay network can be defined similarly to (20).

Since f_i and g_i are independent, for $i = 1, \ldots, R$, the mean value of α^2 is given as

$$\mathbb{E}[\alpha^2] = \sum_{i=1}^{R} \frac{P_i\sigma_{F_i}^2\sigma_{G_i}^2}{P_0\sigma_{F_i}^2 + N_0}. \quad (22)$$

The variance of α^2 is

$$\mathrm{var}[\alpha^2] = \sum_{i=1}^{R} \frac{P_i^2}{\left(P_0\sigma_{F_i}^2 + N_0\right)^2} \mathrm{var}\left[|f_i|^2|g_i|^2\right] = \sum_{i=1}^{R} \frac{3P_i^2\sigma_{F_i}^4\sigma_{G_i}^4}{\left(P_0\sigma_{F_i}^2 + N_0\right)^2} \quad (23)$$

which follows from the fact that $|f_i|^2$ and $|g_i|^2$ are exponentially distributed with means $\sigma_{F_i}^2$ and $\sigma_{G_i}^2$, respectively, and $\mathrm{var}[|f_i|^2|g_i|^2] = \mathbb{E}[|f_i|^4]\mathbb{E}[|g_i|^4] - (\mathbb{E}[|f_i|^2]\mathbb{E}[|g_i|^2])^2 = 2\sigma_{F_i}^4 \times 2\sigma_{G_i}^4 - \sigma_{F_i}^4\sigma_{G_i}^4 = 3\sigma_{F_i}^4\sigma_{G_i}^4$.

Next, observe that the Hölder inequality (see [20, pp. 48]) can be used to obtain the following inequality:

$$\sum_{i=1}^{R} |X_i|^2 \geq \frac{\left(\sum_{i=1}^{R} |X_i|\right)^2}{R} \quad (24)$$

where the equality is achieved when $|X_1| = \cdots = |X_R|$. Then, by applying (24) to (23), one obtains the following lower bound on the variance of α^2:

$$\mathrm{var}[\alpha^2] \geq \frac{3}{R}\left(\sum_{i=1}^{R} \frac{P_i\sigma_{F_i}^2\sigma_{G_i}^2}{P_0\sigma_{F_i}^2 + N_0}\right)^2. \quad (25)$$

Therefore, the amount of fading is lower bounded as

$$\kappa = \frac{\mathrm{var}[\alpha^2]}{\left(\mathbb{E}[\alpha^2]\right)^2} \geq \frac{3}{R} \quad (26)$$

and the lower bound is achieved with

$$\frac{P_1\sigma_{F_1}^2\sigma_{G_1}^2}{P_0\sigma_{F_1}^2 + N_0} = \cdots = \frac{P_R\sigma_{F_R}^2\sigma_{G_R}^2}{P_0\sigma_{F_R}^2 + N_0}. \quad (27)$$

It is noted that the factor 3 in the amount of fading expression for the relay networks is due to the "cascaded" fading characteristic of the AF protocol employed. Furthermore, an amount of fading equal to 1 here does not mean that the system has the diversity order of 1 as in a typical point-to-point communication system over a Rayleigh-fading channel.

D. Optimal PA With the Minimum Amount of Fading Constraint

To minimize the amount of fading of the DSTC in wireless relay networks, the PA scheme between the source and the relays needs to satisfy (27). Apparently, the condition in (27) makes the amount of fading in each $S \rightarrow R \rightarrow D$ link to be the same, which is an intuitively satisfying result. Therefore, the optimization problem of maximizing the average SNR is the same as in (9) but with the additional constraint for the minimum amount of fading as in (27). Intuitively, this optimal power scheme would allocate more power to the relay with a weaker link and less power for the relay with a stronger link. This is reasonable since only channel statistics are known at the relays, and one would like to use all the relay channels reliably to achieve full diversity order.

Define $a = \sum_{i=1}^{R}(1/\sigma_{F_i}^2)$, $b = \sum_{i=1}^{R}(1/\sigma_{G_i}^2)$, and $c = \sum_{i=1}^{R}(N_0/\sigma_{F_i}^2\sigma_{G_i}^2)$. From the minimum amount of fading constraint, one has

$$\frac{P_1}{\frac{P_0\sigma_{F_1}^2+N_0}{\sigma_{F_1}^2\sigma_{G_1}^2}} = \cdots = \frac{P_R}{\frac{P_0\sigma_{F_R}^2+N_0}{\sigma_{F_R}^2\sigma_{G_R}^2}} = \frac{\sum_{i=1}^{R} P_i}{\sum_{i=1}^{R}\frac{P_0\sigma_{F_i}^2+N_0}{\sigma_{F_i}^2\sigma_{G_i}^2}} = \frac{P - P_0}{P_0 b + c} \quad (28)$$

where the condition on optimality in Lemma 1 is used. It follows that

$$P_i = \frac{P - P_0}{P_0 b + c} \cdot \frac{P_0\sigma_{F_i}^2 + N_0}{\sigma_{F_i}^2\sigma_{G_i}^2}, \qquad i = 1, \ldots, R. \quad (29)$$

Substituting $P_1, \ldots, P_R$ from (29) to the objective function in (9), the new objective function can be written as

$$f(P_0) = \frac{1 + \sum_{i=1}^{R} \frac{P-P_0}{(P_0b+c)\sigma_{F_i}^2}}{P_0 R \frac{P-P_0}{P_0b+c}} = \frac{1}{R}\left(\frac{P_0 b + c}{P_0(P - P_0)} + \frac{a}{P_0}\right). \quad (30)$$

Ignoring the constant factor $1/R$, the optimization problem can be simplified to

$$\underset{P_0}{\text{minimize}} \quad f(P_0) = \frac{P_0 b + c}{P_0(P - P_0)} + \frac{a}{P_0}$$
$$\text{subject to} \quad 0 < P_0 < P. \quad (31)$$

Since the second derivative of the objective function is always positive in the domain of P_0, the objective function is convex. This problem can be solved easily, and the solution is given in the following proposition.

Proposition 2: The optimal PA scheme for a relay network that maximizes the effective SNR at the destination under the minimum amount of fading constraint is

$$P_0 = \begin{cases} \frac{\sqrt{(Pa+c)(Pb+c)}-(Pa+c)}{b-a}, & \text{if } b \neq a \\ P/2, & \text{if } b = a \end{cases}$$
$$P_i = \frac{P - P_0}{P_0 b + c} \cdot \frac{P_0\sigma_{F_i}^2 + N_0}{\sigma_{F_i}^2\sigma_{G_i}^2}, \qquad i = 1, \ldots, R \quad (32)$$

where

$$a = \sum_{i=1}^{R} \frac{1}{\sigma_{F_i}^2} \quad b = \sum_{i=1}^{R} \frac{1}{\sigma_{G_i}^2} \quad c = \sum_{i=1}^{R} \frac{N_0}{\sigma_{F_i}^2\sigma_{G_i}^2}.$$

Proposition 2 provides simple closed-form expressions to optimally allocate the total transmitted power in the network to the source and relays. The scheme tries to maximize the effective average SNR at the destination while maintaining a balance between $S \rightarrow R \rightarrow D$ links to minimize the amount of fading. In Section V, it is shown that such a scheme is also optimal in minimizing the upper bound of the SER performance of a proposed DUSTM. It is also noted that as the minimum amount of fading constraint is automatically met with the equal PA at the relays in balanced networks, the closed-form optimal PA scheme for such networks given in (11) is a special case of the expressions in Proposition 2.

IV. Application of Fourier-Based DUSTM in Wireless Relay Networks

This section begins with a brief review of Fourier-based unitary space–time constellation designs for colocated multiple transmit antennas, which was originally proposed in [23]. In this system model, the transmitter is equipped with M antennas, and the channel is assumed to remain constant over T symbol times. The USTM design constructs a constellation of L $T \times M$ unitary matrices $\Phi_1, \ldots, \Phi_L$ such that $\Phi_l^{\mathcal{H}}\Phi_l = \boldsymbol{I}_M$ for $l = 1, \ldots, L$. From this pool of unitary matrices, the transmitted signal matrix is formed as $\sqrt{T}\Phi_l$. Let $\boldsymbol{Y}$ be the received signal matrix. The ML receiver for USTM with *noncoherent reception* was shown in [23] and [24] to be

$$\hat{\Phi} = \arg \max_{\Phi_l = \Phi_1, \ldots, \Phi_L} \operatorname{tr}\left\{\boldsymbol{Y}^{\mathcal{H}}\Phi_l\Phi_l^{\mathcal{H}}\boldsymbol{Y}\right\}. \tag{33}$$

Hochwald *et al.* [23] propose a Fourier-based approach in designing the unitary constellations, which uses ideas from signal processing theory. In this design, the lth constellation point Φ_l can be obtained from the first constellation point Φ_1 as

$$\Phi_l = \Theta^{l-1}\Phi_1 \tag{34}$$

where

$$\Theta = \operatorname{diag}\left[e^{j\frac{2\pi}{L}u_1}, \ldots, e^{j\frac{2\pi}{L}u_T}\right], \quad 0 \le u_1, \ldots, u_T \le L-1 \tag{35}$$

and Φ_1 is constructed by selecting M columns of a $T \times T$ discrete Fourier transform (DFT) matrix. The optimal values of the so-called *frequencies* $u_1, \ldots, u_T$ are also given in [23] for the cases of one, two, and three transmit antennas.

Now, we consider the application of USTM for DSTC in wireless relay networks, where CSI is not available at neither the transmitter nor the receiver, and hence, noncoherent detection is required. First, the lth codeword vector $\boldsymbol{s}_l$ from the source is formed by taking the diagonal elements of matrix Θ^{l-1} and scaling by $1/\sqrt{T}$ to meet the power constraint. That is, $\boldsymbol{s}_l = 1/\sqrt{T}[e^{j(2\pi/L)u_1(l-1)}, \ldots, e^{j(2\pi/L)u_T(l-1)}]^{\mathcal{T}}$. Second, the unitary matrix at each relay is constructed by diagonalizing one of the columns of Φ_1. As an example, the design of Φ_1 for $M = 3$ transmit antennas and $T = 8$ given in [23] is

$$\Phi_1 = \frac{1}{\sqrt{8}}\begin{bmatrix} 1 & 1 & 1 \\ 1 & e^{j\frac{2\pi}{8}5} & e^{j\frac{2\pi}{8}6} \\ 1 & e^{j\frac{2\pi}{8}2} & e^{j\frac{2\pi}{8}4} \\ 1 & e^{j\frac{2\pi}{8}7} & e^{j\frac{2\pi}{8}2} \\ 1 & e^{j\frac{2\pi}{8}4} & 1 \\ 1 & e^{j\frac{2\pi}{8}1} & e^{j\frac{2\pi}{8}6} \\ 1 & e^{j\frac{2\pi}{8}6} & e^{j\frac{2\pi}{8}4} \\ 1 & e^{j\frac{2\pi}{8}3} & e^{j\frac{2\pi}{8}2} \end{bmatrix}.$$

Then, $\boldsymbol{A}_i$'s for a three-relay network are formed as

$$\begin{aligned}
\boldsymbol{A}_1 &= \boldsymbol{I}_8 \\
\boldsymbol{A}_2 &= \operatorname{diag}\left[1, e^{j\frac{2\pi}{8}5}, e^{j\frac{2\pi}{8}2}, e^{j\frac{2\pi}{8}7}, e^{j\frac{2\pi}{8}4}, e^{j\frac{2\pi}{8}1}, e^{j\frac{2\pi}{8}6}, e^{j\frac{2\pi}{8}3}\right] \\
\boldsymbol{A}_3 &= \operatorname{diag}\left[1, e^{j\frac{2\pi}{8}6}, e^{j\frac{2\pi}{8}4}, e^{j\frac{2\pi}{8}2}, 1, e^{j\frac{2\pi}{8}6}, e^{j\frac{2\pi}{8}4}, e^{j\frac{2\pi}{8}2}\right]
\end{aligned}$$

where the normalization factor $1/\sqrt{8}$ is dropped to make $\boldsymbol{A}_i^{\mathcal{H}}\boldsymbol{A}_i = \boldsymbol{I}_8$. With this design, the codeword $\boldsymbol{X}$ in (3) is effectively in the form of (34). Therefore, the noncoherent detection of the codeword vector can be carried out similarly as in (33), where the received signal matrix $\boldsymbol{Y}$ in (33) is substituted by the received signal vector $\boldsymbol{y}$ in (3).

A. ML Receiver for DUSTM Over the Partially Coherent Relay Network

In the partially coherent relay network considered in this paper, the destination has perfect knowledge of all the channels from the relays but not the channels from the source to the relays. This means that g_i is known, while f_i is unknown, for $i = 1, \ldots, R$.

Conditioned on $\{g_i\}$ and the transmitted codeword $\boldsymbol{X}_l$, the received vector $\boldsymbol{y}$ is a circularly symmetric Gaussian vector with covariance matrix

$$\boldsymbol{\Lambda} = \gamma\boldsymbol{I}_T + \boldsymbol{X}_l\boldsymbol{G}\boldsymbol{X}_l^{\mathcal{H}} \tag{36}$$

where $\boldsymbol{G} = \operatorname{diag}(\beta_1|g_1|^2, \ldots, \beta_R|g_R|^2)$, and

$$\beta_i = \frac{P_iP_0T\sigma_{F_i}^2}{P_0\sigma_{F_i}^2 + N_0}, \qquad i = 1, \ldots, R.$$

The received signal has the following conditional probability density function:

$$p\left(\boldsymbol{y}|\boldsymbol{X}_l, \{g_i\}\right) = \frac{\exp(-\boldsymbol{y}^{\mathcal{H}}\boldsymbol{\Lambda}^{-1}\boldsymbol{y})}{\pi^T\det(\boldsymbol{\Lambda})}. \tag{37}$$

Using the property $\det(\boldsymbol{I} + \boldsymbol{AB}) = \det(\boldsymbol{I} + \boldsymbol{BA})$ [25], the determinant of $\boldsymbol{\Lambda}$ can be found as

$$\begin{aligned}
\det(\boldsymbol{\Lambda}) &= \gamma^T\det\left(\boldsymbol{I}_T + \boldsymbol{X}_l\overline{\boldsymbol{G}}\boldsymbol{X}_l^{\mathcal{H}}\right) \\
&= \gamma^T\det(\boldsymbol{I}_R + \overline{\boldsymbol{G}}) \\
&= \gamma^T\prod_{i=1}^{R}\left(1 + \frac{\beta_i}{\gamma}|g_i|^2\right)
\end{aligned}$$

where $\overline{\boldsymbol{G}} = \boldsymbol{G}/\gamma$. Likewise, using the matrix inverse formula [25]

$$(\boldsymbol{A} + \boldsymbol{BCD})^{-1} = \boldsymbol{A}^{-1} - \boldsymbol{A}^{-1}\boldsymbol{B}(\boldsymbol{C}^{-1} + \boldsymbol{DA}^{-1}\boldsymbol{B})^{-1}\boldsymbol{DA}^{-1}$$

the inverse of $\boldsymbol{\Lambda}$ can be calculated as

$$\begin{aligned}
\boldsymbol{\Lambda}^{-1} &= \frac{1}{\gamma}\left(\boldsymbol{I}_T + \boldsymbol{X}_l\overline{\boldsymbol{G}}\boldsymbol{X}_l^{\mathcal{H}}\right)^{-1} \\
&= \frac{1}{\gamma}\left(\boldsymbol{I}_T - \boldsymbol{X}_l\left(\overline{\boldsymbol{G}}^{-1} + \boldsymbol{X}_l^{\mathcal{H}}\boldsymbol{I}_T\boldsymbol{X}_l\right)^{-1}\boldsymbol{X}_l^{\mathcal{H}}\right) \\
&= \frac{1}{\gamma}\left(\boldsymbol{I}_T - \boldsymbol{X}_l\boldsymbol{C}\boldsymbol{X}_l^{\mathcal{H}}\right)
\end{aligned}$$

where

$$\boldsymbol{C} = \operatorname{diag}\left(\frac{\beta_1|g_1|^2}{\gamma + \beta_1|g_1|^2}, \ldots, \frac{\beta_R|g_R|^2}{\gamma + \beta_R|g_R|^2}\right).$$

The partially coherent ML receiver then becomes

$$\begin{aligned} \boldsymbol{X}_{ML} &= \arg \max_{\boldsymbol{X}_l=\boldsymbol{X}_1,\ldots,\boldsymbol{X}_L} p\left(\boldsymbol{y}|\boldsymbol{X}_l,\{g_i\}\right) \\ &= \arg \max_{\boldsymbol{X}_l=\boldsymbol{X}_1,\ldots,\boldsymbol{X}_L} -\frac{1}{\gamma}\boldsymbol{y}^{\mathcal{H}}\left(\boldsymbol{I}_T-\boldsymbol{X}_l\boldsymbol{C}\boldsymbol{X}_l^{\mathcal{H}}\right)\boldsymbol{y} \\ &= \arg \max_{\boldsymbol{X}_l=\boldsymbol{X}_1,\ldots,\boldsymbol{X}_L} \boldsymbol{y}^{\mathcal{H}}\boldsymbol{X}_l\boldsymbol{C}\boldsymbol{X}_l^{\mathcal{H}}\boldsymbol{y}. \end{aligned} \tag{38}$$

B. GLRT Receiver for DUSTM Over the Noncoherent Relay Network

For a (fully) noncoherent relay network, neither the CSI of the relay-to-destination channels nor the CSI of the source-to-relay channels is known. Since each element of $\boldsymbol{h}$ in (3) is a product of two complex Gaussian random variables, the source–relay–destination link is represented by *cascaded* fading. Furthermore, $p(\boldsymbol{y}|\boldsymbol{X}_l)$ does not appear to have a closed-form expression. Thus, it is not trivial to derive the optimal ML receiver for the network. Instead, the suboptimal GLRT receiver [23], [26] shall be considered.

With GLRT, the receiver first estimates the channel $\boldsymbol{h}$ under the hypothesis that the codeword $\boldsymbol{X}_l$ was sent. From (3), conditioned on the transmitted codeword $\boldsymbol{X}_l$, $\{f_i\}$, and $\{g_i\}$, the received vector $\boldsymbol{y}$ is a Gaussian random vector with mean $\boldsymbol{X}_l\boldsymbol{h}$ and covariance matrix $\gamma\boldsymbol{I}_T$, which is the same covariance matrix of the noise vector. Thus, the ML estimation of $\boldsymbol{h}$ is

$$\begin{aligned} \hat{\boldsymbol{h}}_l &= \arg\max_{\boldsymbol{h}} p(\boldsymbol{y}|\boldsymbol{X}_l,\boldsymbol{h}) \\ &= \arg\min_{\boldsymbol{h}} \|\boldsymbol{y}-\boldsymbol{X}_l\boldsymbol{h}\|^2. \end{aligned} \tag{39}$$

It then follows that $\hat{\boldsymbol{h}}_l$ is given by (note that $\boldsymbol{X}_l$ is unitary)

$$\hat{\boldsymbol{h}}_l = \left(\boldsymbol{X}_l^{\mathcal{H}}\boldsymbol{X}_l\right)^{-1}\boldsymbol{X}_l^{\mathcal{H}}\boldsymbol{y} = \boldsymbol{X}_l^{\mathcal{H}}\boldsymbol{y}. \tag{40}$$

Substituting $\hat{\boldsymbol{h}}_l$ into (3), the GRLT receiver is expressed as

$$\begin{aligned} \hat{\boldsymbol{X}}_{\text{GLRT}} &= \arg \max_{\boldsymbol{X}_l=\boldsymbol{X}_1,\ldots,\boldsymbol{X}_L} \left\{-\|\boldsymbol{y}-\boldsymbol{X}_l\hat{\boldsymbol{h}}_l\|^2\right\} \\ &= \arg \max_{\boldsymbol{X}_l=\boldsymbol{X}_1,\ldots,\boldsymbol{X}_L} \boldsymbol{y}^{\mathcal{H}}\boldsymbol{X}_l\boldsymbol{X}_l^{\mathcal{H}}\boldsymbol{y}. \end{aligned} \tag{41}$$

Observe that the GLRT receiver in (41) operates in the same way as the GLRT receiver for colocated multiple transmit antennas in [23] and the receiver for DUSTM with DF relaying protocol in [15] and [16]. Comparing the receiver in (38) for the partially coherent network and the one in (41) for the noncoherent network, it can be seen that the difference is in the existence of the matrix $\boldsymbol{C}$ in the former one. The matrix $\boldsymbol{C}$ contains the CSI of the relay-to-destination channels. However, as the signal power becomes large enough, the matrix $\boldsymbol{C}$ comes closer to an identity matrix, and therefore, the two receivers are basically the same. This observation is reconfirmed in Section V with the pairwise error probability (PEP) analysis.

V. PEP Analysis and Diversity

A. PEP of DUSTM Over the Partially Coherent Relay Network

This section evaluates the PEP performance of partially coherent DUSTM and relates it to the constellation design of DUSTM. Suppose that all the relays are active, which means that the matrix $\boldsymbol{G}$ is full rank. Kiran and Rajan [12] derive the PEP for the partially coherent DUSTM, its Chernoff bound, as well as an approximation for the average SER at the high-SNR region as follows. Suppose that $\boldsymbol{X}_k$ and $\boldsymbol{X}_l$ are two codewords and $\boldsymbol{Z}_{kl} = [\boldsymbol{X}_k, \boldsymbol{X}_l]$ is full rank. Define $\boldsymbol{R}_{kl} = \boldsymbol{X}_k^{\mathcal{H}}\boldsymbol{X}_l$, and let $\boldsymbol{R}_{kk} = \boldsymbol{R}_{ll} = \boldsymbol{K}$. The error probability of decoding to $\boldsymbol{X}_l$ for large η, given that $\boldsymbol{X}_k$ was transmitted, was shown in [12] to be approximated as

$$P_{k,l|\{g_i\}} \approx \frac{\gamma^R}{\det\left(\mu(1-\mu)\boldsymbol{G}\right)}\frac{1}{\det\left(\boldsymbol{K}-\boldsymbol{R}_{lk}\boldsymbol{K}^{-1}\boldsymbol{R}_{kl}\right)} \tag{42}$$

which is minimized with $\mu = 1/2$.

On the other hand, since $\boldsymbol{y}$ is Gaussian distributed and $\boldsymbol{X}_l^{\mathcal{H}}\boldsymbol{C}\boldsymbol{X}_l$ is Hermitian for $l = 1,\ldots,L$, the ML receiver in (38) can be interpreted as a quadratic receiver [27]. The asymptotic PEP performance of the quadratic receiver is readily given as (cf. [27, eq. (28)])

$$P_{k,l|\{g_i\}} = \frac{\gamma^R}{\det(\boldsymbol{G})}\frac{\binom{2R}{R}}{\det\left(\boldsymbol{K}-\boldsymbol{R}_{lk}\boldsymbol{K}^{-1}\boldsymbol{R}_{kl}\right)}. \tag{43}$$

The two aforementioned PEP expressions differ only in scaling factor, and they clearly indicate that the effect of channel coefficients $\{g_i\}$, which are in $\boldsymbol{G}$, can be separated from the effect of the distributed code [12]. In fact, since we are considering DUSTM for partially coherent networks, $\boldsymbol{K} = \boldsymbol{I}_R$, and $\det(\boldsymbol{K}-\boldsymbol{R}_{lk}\boldsymbol{K}^{-1}\boldsymbol{R}_{kl}) = \prod_{r=1}^{R}(1-d_r^2)$, where d_r, $r = 1,\ldots,R$ are the singular values of the correlation matrix $\boldsymbol{X}_k^{\mathcal{H}}\boldsymbol{X}_l$. The PEP will be minimized when this product is maximized. This is the same condition on the constellation design of USTM for colocated transmit antennas in [23]. Therefore, the best Fourier-based constellation design in [23] is also the best Fourier-based constellation design for DUSTM. As shown in [12], the system achieves full diversity order equal to the number of relays if $\boldsymbol{Z}_{kl}$ is full rank for any pair of $\boldsymbol{X}_k$ and $\boldsymbol{X}_l$. The necessary condition for this is $T \geq 2R$, which is similar to the condition imposed in USTM, $T \geq 2M$.

To calculate the symbol error probability, the conditional PEP expression in (42) or (43) has to be averaged over the distribution of $\{g_i\}$. This is analyzed in [12] by performing similar derivation steps for the coherent DSTC in [6]. An important remark from such a PEP analysis is that the SER is proportional to $(\log P/P)^R$ for the balanced networks (with $\sigma_F^2 = \sigma_G^2 = 1$) as P becomes large enough. Thus, DUSTM over a partially coherent relay network is able to achieve full diversity order for very large P, which is the same result obtained for the coherent space–time coding in [6]. However, for an arbitrary network topology, the exact PEP and the diversity order depend on the PA employed. The following lemma establishes the relationship between the optimal PA in Proposition 2 and the PEP of the partially coherent DUSTM.

Lemma 2: Asymptotically, the upper bound on the PEP of partially coherent DUSTM is minimized with the optimal PA scheme under the minimum amount of fading constraint. Maximum diversity order is also obtained by the optimal PA scheme.

Proof: The exact conditional PEP is given in [12] as

$$P_{k,l|\{g_i\}} = \frac{\det(\boldsymbol{I}_R + \boldsymbol{G}/\gamma)}{2\det\left(\boldsymbol{I}_{2R} + \boldsymbol{\Psi}\boldsymbol{Z}_{kl}^{\mathcal{H}}\boldsymbol{Z}_{kl}/(4\gamma)\right)} \tag{44}$$

where $\boldsymbol{\Psi} = \mathrm{diag}(\boldsymbol{G}, \boldsymbol{G})$. To find the unconditional PEP $P_{k,l}$, one needs to average (44) over the distribution of $\{g_i\}$. Since taking the expectation over $\{g_i\}$ is difficult, we take the same approach as in [6] to approximate the random variable γ by its mean value, i.e., $\gamma \approx \bar{\gamma} = N_0(1 + \sum_{i=1}^{R} \varepsilon_i \sigma_{G_i}^2)$. Note that by the law of large number, this approximation holds almost surely as $R \to \infty$. Since $\boldsymbol{Z}_{kl}$ is a full-rank matrix with the Fourier-based USTM design [23], the minimum singular value of $\boldsymbol{Z}_{kl}^{\mathcal{H}}\boldsymbol{Z}_{kl}$, which is denoted as ν^2, is nonzero. Then, the asymptotic PEP $P_{k,l}$ is (approximately) upper bounded as

$$\begin{aligned} P_{k,l} &\lesssim \mathbb{E}_{\{g_i\}} \frac{\det\left(\boldsymbol{I}_R + \boldsymbol{G}/\bar{\gamma}\right)}{2\det\left(\boldsymbol{I}_{2R} + \boldsymbol{\Psi}\nu^2/(4\bar{\gamma})\right)} \\ &= \frac{1}{2}\prod_{i=1}^{R} \mathbb{E}_{\{g_i\}}\left\{\frac{1 + \beta_i |g_i|^2/\bar{\gamma}}{\left[1 + \beta_i \nu^2 |g_i|^2/(4\bar{\gamma})\right]^2}\right\} \\ &= \frac{1}{2}\prod_{i=1}^{R} \int_0^\infty \frac{(1 + a_i x)e^{-x}}{\left(1 + \nu^2 a_i x/4\right)^2} dx \end{aligned} \tag{45}$$

where $a_i = \beta_i \sigma_{G_i}^2/\bar{\gamma}$. Let $1 + \nu^2 a_i x/4 = -\nu^2 a_i t/4$. Then, (45) becomes

$$P_{k,l} \lesssim \frac{1}{2}\left(\frac{16}{\nu^4}\right)^R \prod_{i=1}^{R} \frac{e^{\frac{4}{a_i\nu^2}}}{a_i^2} \int_{-\infty}^{-\frac{4}{a_i\nu^2}} \frac{-a_i t + 1 - 4/\nu^2}{t^2} e^t dt. \tag{46}$$

When $P_0 T/N_0$ becomes large, a_i also becomes large, and $e^{4/(a_i\nu^2)} = 1 + O(4/(a_i\nu^2)) \approx 1$. Furthermore, one has the following approximations when a_i is large:

$$\begin{aligned} \int_{-\infty}^{-\frac{4}{a_i\nu^2}} \frac{-e^t}{t} dt &= -\,\mathrm{Ei}\left(-\frac{4}{a_i\nu^2}\right) = 1 + \log\left(\frac{a_i\nu^2}{4}\right) \\ &\approx \log\left(\frac{a_i\nu^2}{4}\right) \\ \int_{-\infty}^{-\frac{4}{a_i\nu^2}} \frac{e^t}{t^2} dt &= \frac{1}{2}\mathrm{Ei}\left(-\frac{4}{a_i\nu^2}\right) + \frac{a_i\nu^2 e^{-\frac{4}{a_i\nu^2}}}{4} \\ &\approx -\frac{1}{2}\log\left(\frac{a_i\nu^2}{4}\right) + \frac{a_i\nu^2}{4} \end{aligned}$$

where $\mathrm{Ei}(\chi) = \int_{-\infty}^{\chi}(e^t/t)dt$, $\chi < 0$ is the exponential integral function [28]. Clearly, when a_i becomes large, the dominant term of $(e^{4/a_i\nu^2}/a_i^2)\int_{-\infty}^{-(4/a_i\nu^2)}(-a_i t + 1 - 4/\nu^2/t^2)e^t dt$ is $(\log(a_i\nu^2/4)/a_i)$. Thus, the PEP is upper bounded as

$$P_{k,l} \lesssim \frac{1}{2}\left(\frac{4}{\nu^2}\right)^R \prod_{i=1}^{R} \frac{\log(a_i\nu^2/4)}{a_i\nu^2/4}. \tag{47}$$

It can be shown that $\log(\log(t)/t)$ is a convex function[2] for large t [20]. This means that $\log(t)/t$ is a log-convex function for large t, and one has the following inequality:

$$\prod_{i=1}^{R} \frac{\log(t_i)}{t_i} \geq \left[\frac{R\log\left(\sum_{i=1}^{R} t_i/R\right)}{\sum_{i=1}^{R} t_i}\right]^R \tag{48}$$

where the equality holds when $t_1 = \cdots = t_R$. Applying the above inequality into the right-hand side of (47), the upper bound of the PEP is minimized when $a_1 = \cdots = a_R$, i.e., $\beta_1\sigma_{G_1}^2 = \cdots = \beta_R\sigma_{G_R}^2$, which also means that the minimum amount of fading constraint is met. Furthermore, once such a constraint is met, a_i is equal to the average SNR η. Maximizing the SNR under the amount of fading constraint will further minimize the PEP's upper bound. Note that the PEP's upper bound is then proportional to $(\log\eta/\eta)^R$. Thus, the maximum diversity order of DUSTM is obtained by the PA in Proposition 2. ■

B. PEP of DUSTM Over the Noncoherent Relay Network

This section considers the PEP analysis of DUSTM over the noncoherent relay network. Intuitively, the performance of DUSTM over such a network is worse than that over a partially coherent relay network. However, as the total transmit power P becomes very large, it is shown that the two performances are asymptotically the same.

Recall the GLRT receiver in (41). Suppose that the codeword $\boldsymbol{X}_k$ was sent, the PEP of decoding to the wrong codeword $\boldsymbol{X}_l$ is given by

$$P_{k,l} = \Pr\left(\boldsymbol{y}^{\mathcal{H}}\left(\boldsymbol{X}_l\boldsymbol{X}_l^{\mathcal{H}} - \boldsymbol{X}_k\boldsymbol{X}_k^{\mathcal{H}}\right)\boldsymbol{y} > 0|\boldsymbol{X}_k\right). \tag{49}$$

Since $\boldsymbol{y}$ is not Gaussian distributed, (41) cannot be interpreted as a quadratic receiver as in [27]. To calculate the PEP as well as its asymptotic behavior, reintroduce $\{g_i\}$ into the aforementioned equation as follows:

$$P_{k,l} = \mathbb{E}_{\{g_i\}}\underbrace{\left[\Pr\left(\boldsymbol{y}^{\mathcal{H}}\left(\boldsymbol{X}_l\boldsymbol{X}_l^{\mathcal{H}} - \boldsymbol{X}_k\boldsymbol{X}_k^{\mathcal{H}}\right)\boldsymbol{y} > 0|\boldsymbol{X}_k, \{g_i\}\right)\right]}_{\tilde{P}_{k,l|\{g_i\}}}. \tag{50}$$

In other words, $P_{k,l}$ can be obtained by taking the expectation of $\tilde{P}_{k,l|\{g_i\}}$ over $\{g_i\}$ [29].

Conditioned on a specific realization of $\{g_i\}$, $\boldsymbol{y}$ is now Gaussian distributed with zero mean and covariance matrix given in (36). Since $\boldsymbol{X}_l\boldsymbol{X}_l^{\mathcal{H}}$ is Hermitian for $l = 1, \ldots, L$, one

[2]It can easily be verified that $\log(\log(t)/t)$ is convex when $t \geq e^{1+\sqrt{5}/2}$ by its second-order derivative.

can interpret the GLRT receiver as a quadratic receiver. Thus its asymptotic performance is given as (cf. [27, eq. (36)])

$$\tilde{P}_{k,l|\{g_i\}} = \frac{\gamma^R}{\det(\boldsymbol{G})} \frac{\binom{2R-1}{R}\left(1+\frac{\det(\boldsymbol{K})}{\det(\boldsymbol{K})}\right)}{\det\left(\boldsymbol{K}-\boldsymbol{R}_{lk}\boldsymbol{K}^{-1}\boldsymbol{R}_{kl}\right)} = \frac{\gamma^R}{\det(\boldsymbol{G})} \frac{2\binom{2R-1}{R}}{\det\left(\boldsymbol{K}-\boldsymbol{R}_{lk}\boldsymbol{K}^{-1}\boldsymbol{R}_{kl}\right)}. \quad (51)$$

It can be seen that $\tilde{P}_{k,l|\{g_i\}}$ in (51) and $P_{k,l|\{g_i\}}$ in (43) are essentially the same since $2\binom{2R-1}{R} = \binom{2R}{R}$. Thus, conditioned on $\{g_i\}$, the performance of the GLRT receiver for the noncoherent relay network is asymptotically the same as that of the ML receiver for the partially relay network. Interestingly, this fact also makes the constellation design of DUSTM for noncoherent system analogous to the design of the partially coherent DUSTM. Moreover, the optimal PA scheme under the minimum amount of fading constraint is also the optimal one in minimizing the PEP's upper bound of the noncoherent DUSTM at high P. To obtain the average SER $P_{k,l}$ at high P, $\tilde{P}_{k,l|\{g_i\}}$ has to be averaged over the distribution of $\{g_i\}$, which is similar to the process discussed in Section V-A.

C. Impact of Nonfunctioning Relays

In designing a good DSTC, reference [6] points out that the code should be "*scale-free*" in the sense that it should have a large diversity product when one or more of the relays are not functioning. This section investigates the impact of node failures to the performance of the proposed DUSTM and whether the decoding rules for DUSTM are still valid in such situations.

Without loss of generality, it is assumed that the last d relays out of a total of R relays are not working. As the destination knows the channels from the relays in the partially coherent networks, the destination also knows which relay(s) are not working. Recall the decoding rule for partially coherent networks in (38), it can be seen that the last d diagonal elements of matrix $\boldsymbol{C}$ are now zero. Let

$$\boldsymbol{C}' = \operatorname{diag}\left(\frac{\beta_1|g_1|^2}{\gamma+\beta_1|g_1|^2}, \ldots, \frac{\beta_{R-d}|g_{R-d}|^2}{\gamma+\beta_{R-d}|g_{R-d}|^2}\right)$$

which is full rank. Define the $T \times (R-d)$ matrix $\boldsymbol{X}'_l$ that contains the first $R-d$ columns of $\boldsymbol{X}_l$. It is easy to see that $\boldsymbol{X}_l\boldsymbol{C}\boldsymbol{X}_l^{\mathcal{H}} = \boldsymbol{X}'_l\boldsymbol{C}'\boldsymbol{X}_l'^{\mathcal{H}}$. The decoding rule in (38) is then equivalent to

$$\boldsymbol{X}'_{ML} = \arg\max_{\boldsymbol{X}'_1,\ldots,\boldsymbol{X}'_L} \boldsymbol{y}^{\mathcal{H}}\boldsymbol{X}'_l\boldsymbol{C}'\boldsymbol{X}_l'^{\mathcal{H}}\boldsymbol{y}$$

which is the same as the decoding rule for the system with $R-d$ relays. Hence, it is expected that the relay network is able to achieve the diversity order of $R-d$ at very high P.

In noncoherent relay networks, it might not be possible that the destination knows which relay(s) are not working. Since the decoding rule for noncoherent detection in (41) is similar to the decoding rule for the DUSTM using the SR protocol in [15], the analysis on the impact of node failures in our proposed scheme is also similar to that of incorrect decoding and nonforwarding relays with the SR protocol. It was shown in [15] [cf. (9)] that when d out of R relays are not functioning, the PEP derived from the decoding rule (41) decays at the order of $R-d$ for very large SNR. A similar conclusion could be drawn for our proposed noncoherent AF DUSTM. Note that in both the partially coherent and noncoherent receptions, the optimal *frequencies* $u_1, \ldots, u_T$ specifically designed for the network with R relays are no longer optimal for the network with $R-d$ relays. Finally, it should be shown that to achieve the best SER performance of the distributed code from the remaining $R-d$ functioning relays, the optimal PA scheme needs to be adjusted. Such an adjustment can be readily made from the analysis in Section III applied to $R-d$ relays.

VI. Simulation Results

This section presents the simulation results to illustrate the performance of DUSTM for some specific configurations of relay networks that have two or three relays. The data rate is set at 1 bit/channel use. All the channels are assumed to remain constant for $T = 8$. Thus, the codeword $\boldsymbol{X}_l$ is an 8×3 matrix for three relays, or an 8×2 matrix for two relays. The DUSTM constellations are chosen from the optimal designs for two and three transmit antennas [23]. Specifically, the sets of frequencies are $\{1, 7, 60, 79, 187, 125, 198, 154\}$ and $\{220, 191, 6, 87, 219, 236, 173, 170\}$ for two and three relays, respectively. In all simulations, N_0 is normalized to 1.

A. Performance Comparison of DUSTM Over Partially Coherent, Noncoherent, and Coherent Networks

This section compares the performances of DUSTM over different types of relay networks, including partially coherent, noncoherent, and coherent networks. Emphasis shall be given to the comparison between partially coherent and noncoherent networks to illustrate our analysis in Section V. At each value of the total power P, the optimal PA scheme derived in Section III-D is exercised.

Three balanced network configurations are considered, where σ_F^2 and σ_G^2 are used to denote the common variances of $S \rightarrow R$ and $R \rightarrow D$ links, respectively. In the first configuration, the relays are located in the midway between the source and the destination. The variances of the channel coefficients f_i and g_i are set to be unity. As can be seen in Fig. 2, the partially coherent DUSTM outperforms the noncoherent DUSTM in both the two- and three-relay configurations. However, the performance difference is only noticeable at small values of P, i.e., over the low-SNR region. As P increases, the performance curves merge together, which agrees with our asymptotic analysis in previous sections. Another observation is that when P surpasses 18 dB, the DUSTM for the system with three relays starts to perform better than the one with two relays and clearly shows its higher diversity order.

The second simulation investigates the case when the relays are closer to the source than to the destination. This implies that the source-to-relay channels experience a much better condition than the relay-to-destination channels. Specifically, σ_F^2 is

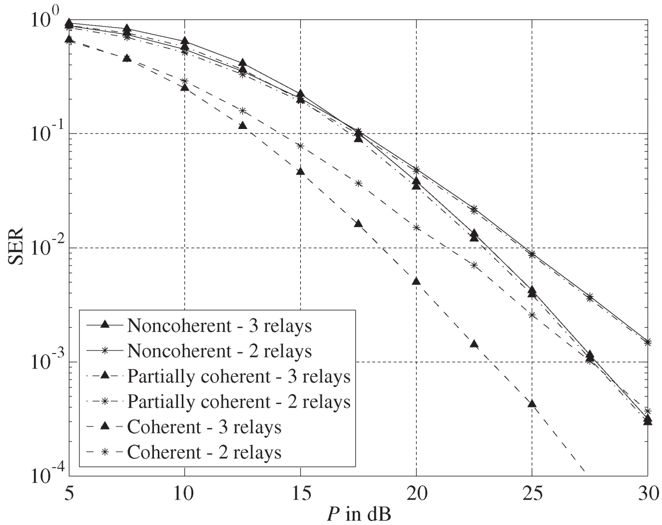

Fig. 2. Symbol error performance of DUSTM with $\sigma_F^2 = 1$ and $\sigma_G^2 = 1$.

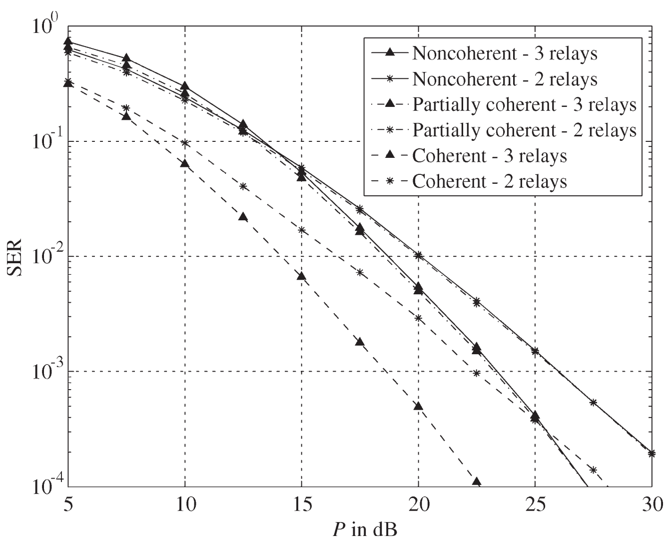

Fig. 3. Symbol error performance of DUSTM with $\sigma_F^2 = 10$ and $\sigma_G^2 = 1$.

assumed to be 10, whereas σ_G^2 is set to 1. The performance of DUSTM in this network configuration is shown in Fig. 3.

The next network configuration considered is the opposite of the second one. The relays are assumed to be closer to the destination than to the source, with $\sigma_F^2 = 1$ and $\sigma_G^2 = 10$. The relay-to-destination channels are relatively much better than the source-to-relay channels. Similar to the first simulation, the performances of DUSTM in Figs. 3 and 4 for the two types of relay networks eventually merge as P becomes large enough. Therefore, it can be concluded that at high SNR, the knowledge of the relay-to-destination channels have no apparent effect on the system performance, no matter how good or poor these channels are compared relative to the source-to-relay channels. Note that since either σ_F^2 or σ_G^2 is increased to 10 in the last two simulations, it requires less total transmit power P to realize the full diversity order of the network.

The performance of the coherent decoder (where the CSI of both source-to-relay and relay-to-destination links are available at the destination) is also presented in Figs. 2 and 3. As can

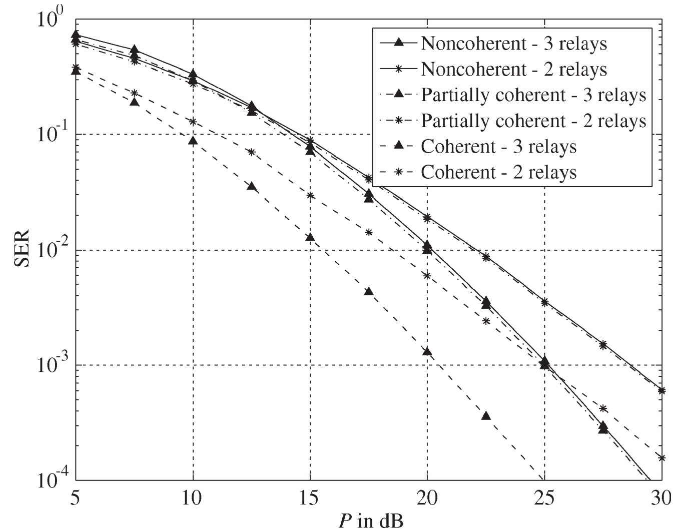

Fig. 4. Symbol error performance of DUSTM with $\sigma_F^2 = 1$ and $\sigma_G^2 = 10$.

be seen in these figures, with the same network configuration, three types of decoders achieve the same diversity order. It is noted that the coherent decoder outperforms the other two decoders by approximately 3–4 dB. This observation is similar to that noted for the performance of USTM in point-to-point communications where the unitary constellations perform about 2–4 dB better when the channel is known, as compared with the case of unknown channel [23].

B. Comparison Between DUSTM and a Random Code

In this section, we compare the performance achieved by the proposed DUSTM with that of a random code, where the third network configuration ($\sigma_F^2 = 1$ and $\sigma_G^2 = 10$) is used as an illustrative example. Instead of using the optimally found *frequencies* $u_1, \ldots, u_T$ for three transmit antennas [23] as in the proposed DUSTM, a random code is formed by randomly generating the *frequencies* with a uniform distribution between 0 and L. The obtained frequencies used in all the simulations are $\{114, 239, 119, 107, 217, 134, 52, 172\}$. Depending on the information bits, the source signals for the random code are formed in a similar process discussed in Section IV. The unitary relay matrices $\boldsymbol{A}_i$ are kept the same as in the proposed DUSTM. As can be seen in Fig. 5, under the partially coherent and noncoherent decoders, the proposed DUSTM outperforms the random code by about 0.5 dB. This performance advantage is due to the use of the optimal *frequencies* designed for the noncoherent USTM. Note, however, that under the coherent decoding rule, the proposed DUSTM performs basically the same as the random code. This is not unexpected since the optimality of the frequencies found in [23] and applied in this paper only holds for partially coherent or noncoherent networks.

Though desirable, it is noted that the optimal *frequencies* in USTM can only be found by an exhaustive searching process [23], which is not practically attractive when the number of relays is large and when the transmission interval T in DUSTM is varied. On the other hand, the relatively good performance of random codes makes them a viable option in designing DUSTM. More specifically, the source signal is simply formed

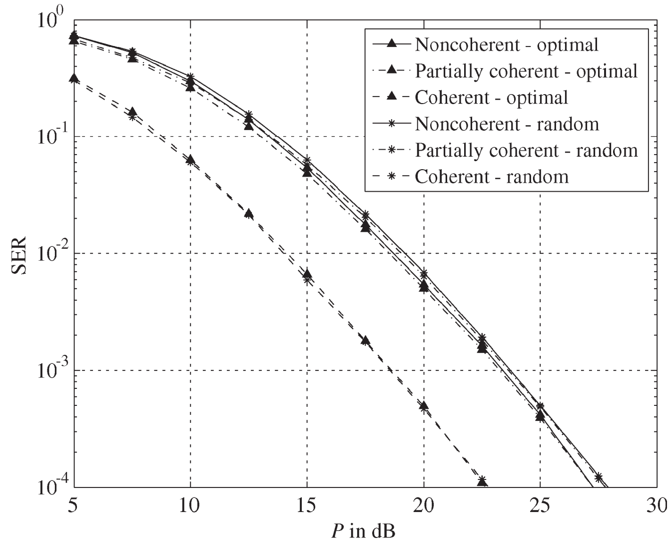

Fig. 5. Symbol error performances of the proposed DUSTM and a random code with $\sigma_F^2 = 1$ and $\sigma_G^2 = 10$.

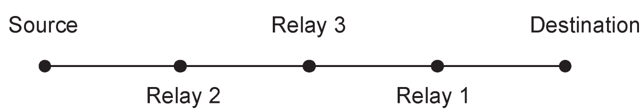

Fig. 6. Relay locations relative to the source and destination.

from randomly chosen *frequencies*, while the relay matrices $\boldsymbol{A}_i$ are formed by selecting columns of DFT matrices of size $T \times T$.

C. Impact of PA Schemes

This section presents numerical results of the PA schemes in unbalanced networks (see Fig. 6). Assume that the source and destination are located at (0, 0) and (1, 0). In this work, the location of each relay can be anywhere between the source and the destination. Here, we assume that the first relay is located at three quarters away from the source, i.e., location (0.75, 0), and the second relay is at (0.25, 0). The location of the third relay, if deployed, is at midway between the source and the destination, i.e., (0.5, 0). The fading variances are assigned proportionally to the distance between the transmit and receive terminals, taking into account the path loss exponent, which is set at 4. Thus, if $\sigma_{F_1}^2$ is normalized to 1, then $\sigma_{F_2}^2 = 3^4$, and $\sigma_{F_3}^2 = (3/2)^4$. Similarly, $\sigma_{G_1}^2 = 3^4$, $\sigma_{G_2}^2 = 1$, and $\sigma_{G_3}^2 = (3/2)^4$.

Fig. 7 illustrates the effective average SNR at the destination with the following three PA schemes: 1) optimal PA with the minimum amount of fading constraint (AoF const.); 2) optimal PA without the amount of fading constraint; and 3) equal PA. The average SNR values are calculated by both the exact evaluation given in (7) and the approximation given in (8). A network with three relays is considered. As can be seen in the figure, given the total power budget P, the optimal PA without the amount of fading constraint scheme gives the highest SNR, which is followed by the optimal PA scheme with the minimum amount of fading constraint. However, there is only one active relay, i.e., the third relay, in the optimal PA with no amount of fading constraint. Therefore, although achieving the highest average SNR, having only one active relay leads to a decrease in the diversity order (as illustrated in Fig. 8). Furthermore, in comparing the approximate average SNR to the exact average SNR, Fig. 7 shows that the approximation taken in (8) is very accurate, particularly in PA schemes where all the relays are active. Interestingly, the two evaluations of the average SNR for the optimal PA with the amount of fading constraint scheme are almost identical (they cannot be distinguished from the figure).

To illustrate the SER performance of different PA schemes, networks with two relays (relays 1 and 2) and three relays and noncoherent detection are considered. Fig. 8 shows a significant improvement of the optimal PA scheme under the minimum amount of fading constraint over the equal PA scheme, where the former one outperforms the latter by 4 and 2.5 dB in the three- and two-relay networks, respectively. Observe that full diversity order is obtained with the optimal PA scheme. In contrast, with only one relay active when exercising the optimal PA scheme with no amount of fading constraint, the DUSTM in

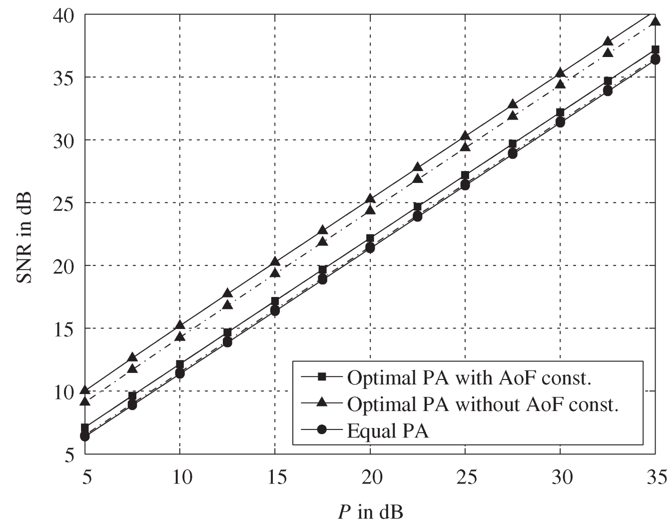

Fig. 7. Effective average SNR at the destination with different PA schemes. ("Dash–dot" lines) Exact SNR. (Solid lines) SNR evaluated by (8).

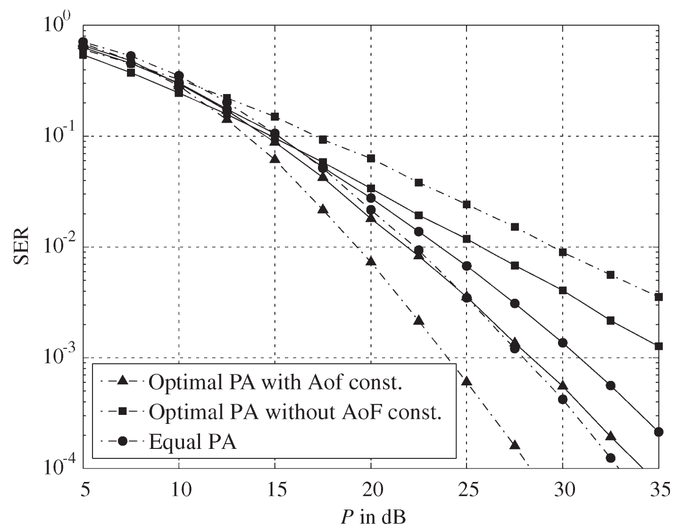

Fig. 8. Performance of noncoherent DUSTM with different PA schemes. ("Dash–dot" lines) Three-relay system. (Solid lines) Two-relay system.

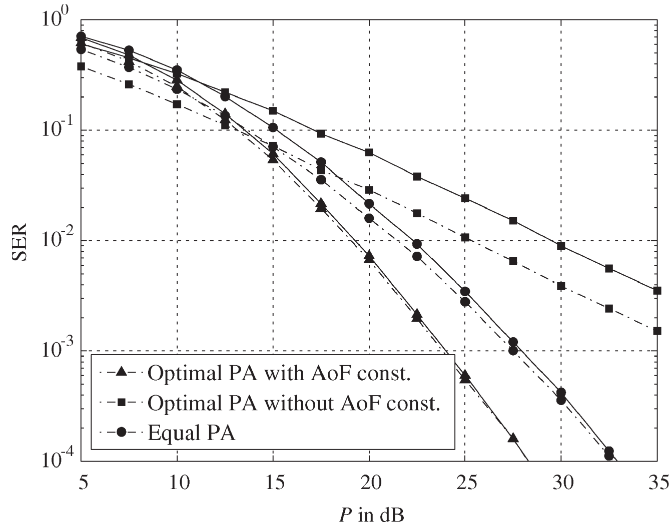

Fig. 9. Performance of DUSTM for a three-relay network with different types of detections and PA schemes. ("Dash–dot" lines) Partially coherent detections. (Solid lines) Noncoherent detections.

both relay networks can offer a diversity of 1 only, leading to a much poorer error performance at high SNR.

Finally, Fig. 9 displays the performances of the partially coherent and noncoherent detections of DUSTM with different PA schemes in an unbalanced three-relay network. As can be seen in the figure, when all the relays are active (under the optimal PA with the amount of fading constraint and equal PA schemes), the SER performances of the two decoding schemes eventually merge at high P. This agrees with our analysis in Section V. It is noted that the asymptotic performances of the two decoding schemes do not match when only one relay is active under the optimal PA with no amount of fading constraint. Furthermore, both decoding schemes do not collapse with one active relay, hence, showing the "*scale-free*" characteristic of the proposed DUSTM. A similar observation holds for the performances of the two decoding schemes under different PA schemes in the two-relay network.

VII. Conclusion

This paper has derived a new optimal PA scheme to maximize the effective average SNR at the destination of a wireless relay network while minimizing the amount of fading experienced with the network. The derivation allows the relays to be anywhere between the source and destination and applies to both types of relay networks considered: partially coherent (i.e., the relays do not know any channels while the destination knows the relay-to-destination channels) and noncoherent (i.e., the relays and destination do not know any channels). The application of Fourier-based DUSTM in wireless relay networks was also presented. The ML receiver for the partially coherent DUSTM and the GLRT receiver for the noncoherent DUSTM were developed. The performances of the two receivers were analyzed, and it was shown that they are asymptotically the same. Simulation results illustrated significant performance improvements achieved by the proposed optimal PA scheme when applied for DUSTM over both types of networks.

Acknowledgment

The authors would like to thank the anonymous reviewers for their helpful comments, which significantly improved the presentation of this paper.

References

[1] A. Sendonaris, E. Erkip, and B. Aazhang, "User cooperation diversity—Part I: System description," *IEEE Trans. Commun.*, vol. 51, no. 11, pp. 1927–1938, Nov. 2003.

[2] J. N. Laneman, D. N. C. Tse, and G. W. Wornell, "Cooperative diversity in wireless networks: Efficient protocols and outage behavior," *IEEE Trans. Inf. Theory*, vol. 50, no. 12, pp. 3062–3080, Dec. 2004.

[3] M. Dohler, "Virtual antenna arrays," Ph.D. dissertation, King's College London, London, U.K., 2003.

[4] J. N. Laneman and G. W. Wornell, "Distributed space–time-coded protocols for exploiting cooperative diversity in wireless networks," *IEEE Trans. Inf. Theory*, vol. 49, no. 10, pp. 2415–2425, Oct. 2003.

[5] R. U. Nabar, H. Bolcskei, and F. W. Kneubuhler, "Fading relay channels: Performance limits and space–time signal design," *IEEE J. Sel. Areas Commun.*, vol. 22, no. 6, pp. 1099–1109, Aug. 2004.

[6] Y. Jing and B. Hassibi, "Distributed space–time coding in wireless relay networks," *IEEE Trans. Wireless Commun.*, vol. 5, no. 12, pp. 3524–3536, Dec. 2006.

[7] Y. Jing and H. Jafarkhani, "Using orthogonal and quasi-orthogonal designs in wireless relay networks," *IEEE Trans. Inf. Theory*, vol. 53, no. 11, pp. 4106–4118, Nov. 2007.

[8] S. Yiu, R. Schober, and L. Lampe, "Distributed space–time block coding," *IEEE Trans. Commun.*, vol. 54, no. 7, pp. 1195–1206, Jul. 2006.

[9] P. Tarasak, H. Minn, and V. K. Bhargava, "Differential modulation for two-user cooperative diversity systems," *IEEE J. Sel. Areas Commun.*, vol. 23, no. 9, pp. 1891–1900, Sep. 2005.

[10] D. Chen and J. N. Laneman, "Modulation and demodulation for cooperative diversity in wireless systems," *IEEE Trans. Wireless Commun.*, vol. 5, no. 7, pp. 1785–1794, Jul. 2006.

[11] H. Mheidat and M. Uysal, "Non-coherent and mismatched-coherent receivers for distributed STBCs with amplify-and-forward relaying," *IEEE Trans. Wireless Commun.*, vol. 6, no. 11, pp. 4060–4070, Nov. 2007.

[12] T. Kiran and B. S. Rajan, "Partially-coherent distributed space–time codes with differential encoder and decoder," *IEEE J. Sel. Areas Commun.*, vol. 25, no. 2, pp. 426–433, Feb. 2007.

[13] F. Oggier and B. Hassibi, "A coding scheme for wireless networks with no channel information," in *Proc. Allerton Conf. Commun. Control Comput.*, Sep. 2006, pp. 113–117.

[14] F. Oggier and B. Hassibi, *Cyclic distributed space–time codes for wireless networks with no channel information*, Mar. 2007. to be published. [Online]. Available: http://www.systems.caltech.edu/~frederique/submitDSTCnoncoh.pdf

[15] T. Wang, Y. Yao, and G. B. Giannakis, "Non-coherent distributed space–time processing for multiuser cooperative transmissions," *IEEE Trans. Wireless Commun.*, vol. 5, no. 12, pp. 3339–3343, Dec. 2006.

[16] S. Yiu, R. Schober, and L. Lampe, "Noncoherent distributed space time block coding," in *Proc. IEEE 62nd VTC—Fall*, Sep. 2005, vol. 2, pp. 947–951.

[17] Y. Li, B. Vucetic, Z. Zhou, and M. Dohler, "Distributed adaptive power allocation for wireless relay networks," *IEEE Trans. Wireless Commun.*, vol. 6, no. 3, pp. 948–958, Mar. 2007.

[18] J. Stoer and R. Bulirsh, *Introduction To Numerical Analysis*. New York: Springer-Verlag, 2002.

[19] P. H. Gregson, "Using angular dispersion of gradient direction for detecting edge ribbons," *IEEE Trans. Pattern Anal. Mach. Intell.*, vol. 15, no. 7, pp. 682–696, Jul. 1993.

[20] S. Boyd and L. Vandenberghe, *Convex Optimization*. Cambridge, U.K.: Cambridge Univ. Press, 2004.

[21] M. K. Simon and M.-S. Alouini, *Digital Communication Over Fading Channels: A Unified Approach to Performance Analysis*. New York: Wiley, 2000.

[22] B. Holter and G. E. Oien, "On the amount of fading in MIMO diversity system," *IEEE Trans. Wireless Commun.*, vol. 4, no. 5, pp. 2498–2507, Sep. 2005.

[23] B. M. Hochwald, T. L. Marzetta, T. J. Richardson, W. Sweldens, and R. Urbanke, "Systematic design of unitary space–time constellations," *IEEE Trans. Inf. Theory*, vol. 46, no. 6, pp. 1099–1109, Sep. 2000.

[24] B. M. Hochwald and T. L. Marzetta, "Unitary space–time modulation for multiple-antenna communications in Rayleigh flat fading," *IEEE Trans. Inf. Theory*, vol. 46, no. 2, pp. 543–564, Mar. 2000.

[25] R. A. Horn and C. R. Johnson, *Matrix Analysis*. New York: Cambridge Univ. Press, 1985.
[26] H. L. Van Trees, *Detection, Estimation, and Modulation Theory—Part I*. New York: Wiley, 1968.
[27] M. Brehler and M. K. Varanasi, "Asymptotic error probability analysis of quadratic receivers in Rayleigh-fading channels with applications to a unified analysis of coherent and noncoherent space–time receivers," *IEEE Trans. Inf. Theory*, vol. 47, no. 6, pp. 2383–2399, Sep. 2001.
[28] I. S. Gradshteyn and I. M. Ryzhik, *Table of Integrals, Series, and Products*, 7th ed. New York: Academic, 2007.
[29] A. Papoulis and S.U. Pillai, *Probability, Random Variables and Stochastic Processes*, 4th ed. Boston, MA: McGraw-Hill, 2002.

Duy H. N. Nguyen (S'07) received the B.Eng. degree (with first-class honors) from Swinburne University of Technology, Hawthorn, Australia, in 2005. He is currently working toward the M.Sc. degree in electrical engineering with the Department of Electrical Engineering, University of Saskatchewan, Saskatoon, SK, Canada.

His research interests include resource allocation in relay networks, convex optimization, and game theory.

Mr. Nguyen was a recipient of the Australian Development Scholarship (ADS) for his undergraduate study in Australia.

Ha H. Nguyen (M'01–SM'05) received the B.Eng. degree in electrical engineering from Hanoi University of Technology, Hanoi, Vietnam, in 1995, the M.Eng. degree in electrical engineering from the Asian Institute of Technology, Bangkok, Thailand, in 1997, and the Ph.D. degree in electrical engineering from the University of Manitoba, Winnipeg, MB, Canada, in 2001.

He joined the Department of Electrical Engineering, University of Saskatchewan, Saskatoon, SK, Canada, in 2001, where he became a Full Professor in 2007. He holds adjunct appointments with the Department of Electrical and Computer Engineering, University of Manitoba, Winnipeg, MB, Canada, and TRLabs, Saskatoon, and was a Senior Visiting Fellow with the School of Electrical Engineering and Telecommunications, University of New South Wales, Sydney, Australia, from October 2007 to June 2008. His research interests include digital communications, spread-spectrum systems, and error-control coding.

Dr. Nguyen currently serves as an Associate Editor for the IEEE TRANSACTIONS ON WIRELESS COMMUNICATIONS and the IEEE TRANSACTIONS ON VEHICULAR TECHNOLOGY. He is a Registered Member of the Association of Professional Engineers and Geoscientists of Saskatchewan.

Hoang Duong Tuan (M'95) was born in Hanoi, Vietnam, in 1964. He received the B.S. and the Ph.D. degrees in applied mathematics from Odessa State University, Odessa, Ukraine, in 1987 and 1991, respectively.

From 1991 to 1994, he was a Researcher with the Optimization and Systems Division, Vietnam National Center for Science and Technologies. He spent nine academic years in Japan as an Assistant Professor with the Department of Electronic–Mechanical Engineering, Nagoya University, Nagoya, Japan, from 1994 to 1999 and then as an Associate Professor with the Department of Electrical and Computer Engineering, Toyota Technological Institute, Nagoya, from 1999 to 2003. He is currently an Associate Professor with the School of Electrical Engineering and Telecommunications, University of New South Wales, Sydney, NSW, Australia. His research interests include theoretical developments and applications of optimization-based methods in many areas of control, signal processing, communication, and bio-informatics.